

PROCEEDINGS
TWENTY-FIRST WORKSHOP
GEOHERMAL RESERVOIR
ENGINEERING

January 22-24, 1996



**Stanford Geothermal Program
Workshop Report SGP-TR-151**

DISCLAIMER

This report was prepared as an account of work sponsored by an agency of the United States Government. Neither the United States Government nor any agency Thereof, nor any of their employees, makes any warranty, express or implied, or assumes any legal liability or responsibility for the accuracy, completeness, or usefulness of any information, apparatus, product, or process disclosed, or represents that its use would not infringe privately owned rights. Reference herein to any specific commercial product, process, or service by trade name, trademark, manufacturer, or otherwise does not necessarily constitute or imply its endorsement, recommendation, or favoring by the United States Government or any agency thereof. The views and opinions of authors expressed herein do not necessarily state or reflect those of the United States Government or any agency thereof.

DISCLAIMER

Portions of this document may be illegible in electronic image products. Images are produced from the best available original document.

PERMEABILITY, ELECTRICAL IMPEDANCE, AND ACOUSTIC VELOCITIES ON RESERVOIR ROCKS FROM THE GEYSERS GEOTHERMAL FIELD

G. N. BOITNOTT AND P. J. BOYD

New England Research, Inc.
76 Olcott Drive
White River Junction, VT, 05001

ABSTRACT

Previous measurements of acoustic velocities on NEGU-17 cores indicate that saturation effects are significant enough to cause V_p/V_s anomalies observed in the field. In this study we report on the results of new measurements on core recently recovered from SB-15-D along with some additional measurements on the NEGU-17 cores. The measurements indicate correlations between mechanical, transport, and water storage properties of the matrix which may prove useful for reservoir assessment and management. The SB-15-D material is found to be similar to the NEGU-17 material in terms of acoustic velocities, being characterized by a notably weak pressure dependence on the velocities and a modest V_p/V_s signature of saturation. The effect of saturation on V_p/V_s appears to result in part from a chemo-mechanical weakening of the shear modulus due to the presence of water. Electrical properties of SB-15-D material are qualitatively similar to those of the NEGU-17 cores, although resistivities of SB-15-D cores are notably lower and dielectric permittivities higher than in their NEGU-17 counterparts.

While some limited correlations of measured properties with depth are noted, no clear change in character is observed within SB-15-D cores which can be associated with the proposed cap-rock/reservoir boundary.

I. INTRODUCTION

Over the last two years, a suite of laboratory measurements have been conducted on Geysers rocks recovered from reservoir depths in NEGU-17. One of the main discoveries of this work has been the observation that the presence of water causes a reduction in the dynamic shear modulus. This frame-weakening is one of the primary effects of saturation on the mechanical properties. While saturation effects on matrix velocities are relatively small, it has been shown that they are capable of producing the V_p/V_s anomalies observed in the field [see *Boitnott*, 1995]. These field scale anomalies have been interpreted to reflect undersaturation in the reservoir [*O'Connell and Johnson*, 1991].

Recently, The Geysers Coring Project in SB-15-D has added significantly to the amount of reservoir core available for testing. This material provides us with an excellent opportunity to further our understanding of the properties of the reservoir matrix with the goal of improving our capabilities in the assessment and prediction of reservoir performance at The Geysers. The SB-15-D material allows us to determine if the patterns observed from experiments on the NEGU-17 core are representative of the reservoir as a whole. Additionally, since the core spans the transition from cap-rock to reservoir, the SB-15-D core is well suited for exploring the nature of the cap-rock/reservoir boundary.

Samples from SB-15-D have been tested using a suite of experiments identical to those performed on the NEGU-17 cores. Complex electrical impedance has also been measured on all SB-15-D and NEGU-17 samples in an attempt to find correlations between electrical properties and velocities. Additionally, permeability versus effective confining pressure has been measured on NEGU-17 metagraywackes, and complex electrical impedance has been measured as a function of saturation on selected metagraywackes from NEGU-17.

The resulting integrated data-set is a valuable tool for constructing models of mechanical and transport properties of The Geysers matrix. With a sufficient understanding of the mechanical, transport, and electrical properties, we hope to be able to assess the use of geophysical methods for predicting and monitoring reservoir performance as well as for delineating the cap-rock/reservoir boundary. An understanding of the physical processes that cause the interrelationships between fundamental matrix properties is central to interpretations of saturation effects and their possible detection using field seismic and other geophysical measurements.

II. SAMPLE SELECTION AND DESCRIPTION

Tests were performed on 17 samples from 11 depths in SB-15-D and 8 samples from 4 depths in NEGU-17. The samples were selected to obtain representative and uniform pieces of the intact matrix material, as well as to represent the range of

lithologies prevalent in the reservoir. The samples from SB-15-D range in depth from 266.7 m to 483.1 m, which spans the proposed caprock/reservoir boundary. A discussion of the petrography of the SB-15-D core and its geologic context has been given by *Hulen and Nielson* [1995]. A description of the NEGU-17 samples (along with supporting measurements) is provided by *Boitnott* [1995].

Lithology, bulk densities (dry and saturated), and inferred porosities and grain densities (based on dry and saturated densities) for the SB-15-D samples are given in Table I. Porosities range from 0.6 to 3.9 percent, with argillites having higher porosities than the metagraywackes. Grain densities of metagraywacke samples are confined to a limited range of 2.69 to 2.71 g/cc. Grain densities of argillite samples are more variable (and in general higher than those of the metagraywackes), ranging from 2.72 to 2.84 g/cc. The grain densities and porosities of the SB-15-D samples are remarkably similar to those of the NEGU-17 cores [see *Boitnott*, 1995], indicating the similarity of their petrographic character.

III. ULTRASONIC VELOCITIES

Ultrasonic compressional and shear velocities were measured on all samples, both dry and saturated with distilled water. Measurements were made during loading and unloading to effective confining pressures from 2 to 90 MPa at ambient pore pressure.

The effects of pressure and saturation on the velocities are quite similar to those found previously for the NEGU-17 cores. Examples of results from two samples are shown in Figure 1. In general there is very little pressure effect on the velocities, a characteristic rather unique to The Geysers material.

Velocities of the SB-15-D samples (at 30 MPa effective confining stress) are summarized in Table II. A clear reduction in the dynamic shear modulus with saturation is apparent in nearly all samples, the effect being larger among argillites than among metagraywackes. As within the NEGU-17 data-set, among SB-15-D metagraywackes, shear velocity reduction with saturation varies from negligible to nearly 5%. Shear velocity reduction among SB-15-D argillites is much stronger than that observed in NEGU-17, with reductions ranging from 5% to 11%. In both the metagraywackes and the argillites, these reductions in shear velocity with saturation are far in excess of what can be accounted for from the slight increase in bulk density. This suggests that the presence of water causes a chemo-mechanical weakening of the shear modulus.

In all samples, saturation increases the dynamic bulk modulus and decreases the dynamic shear modulus. As with the NEGU-17 material, the

effects of saturation can be modeled using a modified low-frequency Biot theory [see *Boitnott* 1995]. This assumes that saturation causes two effects, a stiffening of the dynamic bulk modulus as predicted by Biot's low frequency theory [*Biot*, 1956], and a reduction in the dynamic shear modulus (as a result of chemo-mechanical weakening at grain contacts and/or of mineral phases). According to the model, the saturated bulk modulus (K_{sat}) is given by

$$K_{sat} = K_{dry} + \Delta K \quad (1a)$$

where ΔK represents the increase in bulk modulus due to saturation as described by Biot's low frequency poroelastic theory, and is given by

$$\Delta K = \frac{(K_{solid} - K_{dry})^2}{K_{solid} [1 - \phi - (K_{dry}/K_{solid}) + \phi(K_{solid}/K_f)]} \quad (1b)$$

ΔK is a function of the porosity (ϕ), the bulk moduli of the fluid (K_f) and the solid (K_{solid}) comprising the matrix, and the bulk modulus of the dry matrix itself (K_{dry}). In this modified model, the shear modulus G is assumed to weaken with saturation

$$G_{sat} = G_{dry} - \Delta G \quad (1c)$$

Note that in fitting the model to the velocity data (and using bulk properties in Table I), there are only two free parameters, ΔG and K_{solid} . Example fits of data with the model, assuming that ΔG is independent of confining stress, are shown in Figure 1. Preliminary inversions of the data indicate that ΔG ranges from 0.7 to 2.2 GPa in SB-15-D metagraywackes and K_{solid} ranges from 47 to 53 GPa. SB-15-D argillites exhibit more variation in these properties, with ΔG ranging from 2.5 to 5.5 GPa and K_{solid} varying from 38 to 70 GPa. Interestingly, in some of the argillites from SB-15-D, the shear modulus weakening with saturation is large enough (in comparison to the stiffening effects on the bulk modulus), to result in a net decrease in V_p with saturation.

A summary plot of velocity data for both SB-15-D and NEGU-17 is shown in Figure 2. In general, saturated compressional and shear velocities of SB-15-D samples are slightly lower than those measured on NEGU-17 samples. Dry shear velocities also exhibit this pattern, but dry compressional velocities of SB-15-D cores are not clearly distinguishable from those of NEGU-17 samples (dry velocity data not shown).

In Figure 2, a negative correlation between compressional and shear velocities (at 30 MPa effective confining stress) with porosity (at room pressure) is apparent. Among SB-15-D cores, argillite samples exhibit higher porosity and generally lower velocities than metagraywackes. Note how-

| Table I | | | | | | |
|---------------------------|---------------|------------|---------------------|---------------------------|---------------|-----------------------|
| Bulk Properties (SB-15-D) | | | | | | |
| Plug | Lithology | Depth m | Dry Density g/cc | Saturated Density g/cc | Porosity % | Grain Density g/cc |
| 875 | metagraywacke | 266.7 | 2.622 | 2.647 | 2.5 | 2.689 |
| 1038 | metagraywacke | 316.6 | 2.650 | 2.672 | 2.2 | 2.710 |
| 1070 | argillite | 326.3 | 2.619 | 2.658 | 3.9 | 2.725 |
| 1245_s1 | metagraywacke | 379.6 | 2.702 | 2.708 | 0.6 | 2.718 |
| 1245_s2 | metagraywacke | 379.6 | 2.698 | 2.707 | 0.9 | 2.722 |
| 1279_s1 | metagraywacke | 390.0 | 2.669 | 2.688 | 1.9 | 2.721 |
| 1384_s1 | metagraywacke | 421.8 | 2.651 | 2.670 | 1.9 | 2.702 |
| 1384_s2 | metagraywacke | 421.8 | 2.650 | 2.669 | 1.9 | 2.701 |
| 1442_s1 | argillite | 439.7 | 2.674 | 2.706 | 3.2 | 2.762 |
| 1442_s2 | argillite | 439.7 | 2.687 | 2.726 | 3.9 | 2.796 |
| 1460 | metagraywacke | 445.0 | 2.657 | 2.670 | 1.3 | 2.692 |
| 1492_s1 | argillite | 454.9 | 2.721 | 2.755 | 3.4 | 2.817 |
| 1492_s2 | argillite | 454.9 | 2.751 | 2.784 | 3.3 | 2.845 |
| 1553_s1 | argillite | 473.5 | 2.674 | 2.702 | 2.8 | 2.751 |
| 1553_s2 | argillite | 473.5 | 2.686 | 2.714 | 2.8 | 2.763 |
| 1585_s1 | metagraywacke | 483.3 | 2.683 | 2.693 | 1.0 | 2.710 |
| 1585_s2 | metagraywacke | 483.3 | 2.684 | 2.694 | 1.0 | 2.711 |

| Table II | | | | | | | | | |
|--|--------------|--------------|-----------|--------------|--------------|-----------|-------------------------|-------------------------|---|
| Velocities @ 30 MPa Effective Pressure (SB-15-D) | | | | | | | | | |
| Plug | Dry | | | Saturated | | | Effect of Saturation | | |
| | V_p m/s | V_s m/s | V_p/V_s | V_p m/s | V_s m/s | V_p/V_s | $\Delta V_p/V_p _{dry}$ | $\Delta V_s/V_s _{dry}$ | $\frac{\Delta(V_p/V_s)}{(V_p/V_s)_{dry}}$ |
| 875 | 5061 | 3131 | 1.616 | 5167 | 3050 | 1.694 | 0.021 | -0.026 | 0.048 |
| 1038 | 5131 | 3158 | 1.625 | 5275 | 3030 | 1.741 | 0.028 | -0.041 | 0.072 |
| 1070 | 4814 | 2832 | 1.700 | 4662 | 2590 | 1.800 | -0.032 | -0.085 | 0.059 |
| 1245_s1 | 5445 | 3253 | 1.674 | 5565 | 3145 | 1.769 | 0.022 | -0.033 | 0.057 |
| 1245_s2 | 5528 | 3283 | 1.684 | 5591 | 3151 | 1.774 | 0.011 | -0.040 | 0.054 |
| 1279_s1 | 5343 | 3226 | 1.656 | 5269 | 3158 | 1.668 | -0.014 | -0.021 | 0.007 |
| 1384_s1 | 5403 | 3220 | 1.678 | 5454 | 3140 | 1.737 | 0.009 | -0.025 | 0.035 |
| 1384_s2 | 5357 | 3222 | 1.663 | 5384 | 3105 | 1.734 | 0.005 | -0.036 | 0.043 |
| 1442_s1 | 5112 | 3174 | 1.611 | 5206 | 2913 | 1.787 | 0.018 | -0.082 | 0.109 |
| 1442_s2 | 4848 | 3125 | 1.551 | 4901 | 2844 | 1.723 | 0.011 | -0.090 | 0.111 |
| 1460 | 5539 | 3305 | 1.676 | 5534 | 3201 | 1.729 | -0.001 | -0.032 | 0.032 |
| 1492_s1 | 5345 | 2971 | 1.799 | 5272 | 2648 | 1.991 | -0.014 | -0.109 | 0.107 |
| 1492_s2 | 5180 | 2993 | 1.731 | 5154 | 2771 | 1.860 | -0.005 | -0.074 | 0.075 |
| 1553_s1 | 4805 | 2994 | 1.605 | 5035 | 2809 | 1.792 | 0.048 | -0.062 | 0.117 |
| 1553_s2 | 4739 | 2864 | 1.654 | 4835 | 2669 | 1.812 | 0.020 | -0.068 | 0.095 |
| 1585_s1 | 5568 | 3280 | 1.697 | 5561 | 3154 | 1.763 | -0.001 | -0.038 | 0.039 |
| 1585_s2 | 5569 | 3264 | 1.705 | 5537 | 3199 | 1.731 | -0.006 | -0.020 | 0.015 |

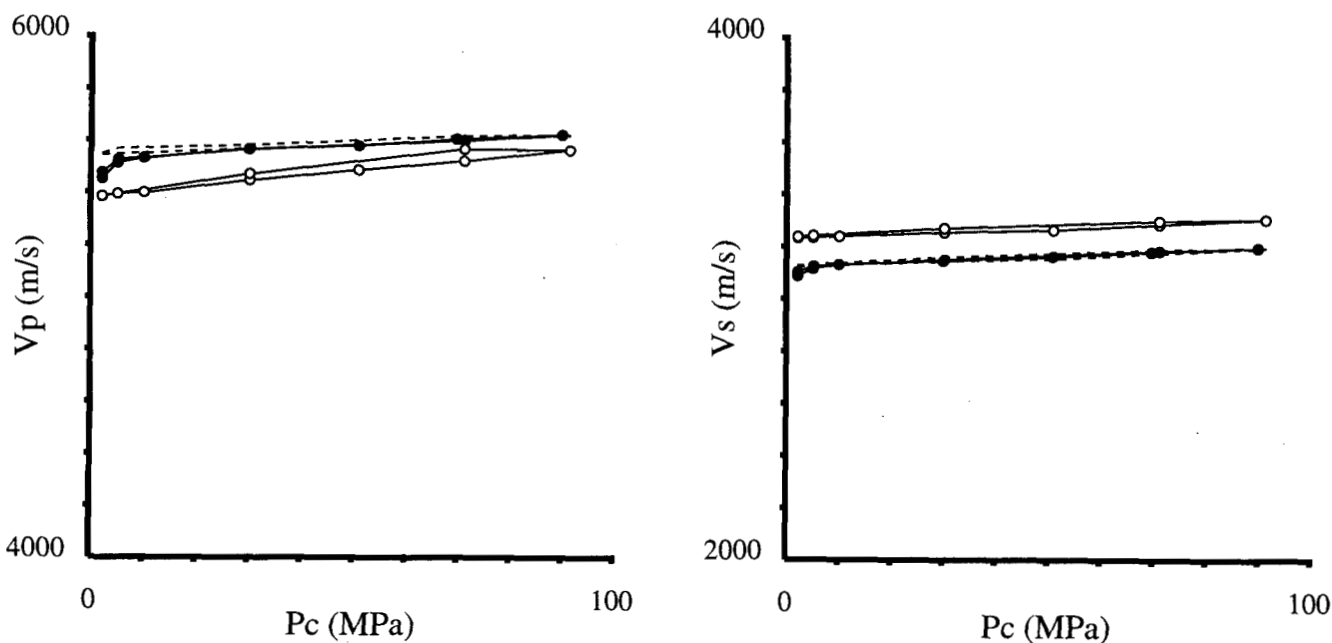


Figure 1a: Compressional and shear velocities as a function of effective confining pressure for metagraywacke plug 1245_s1. Open circles indicate dry and solid circles indicate saturated. The dashed lines are the best fitting model predictions of saturated velocities (based on dry velocities, equations 1a-c, and the bulk properties in Table I), with $\Delta G = 1.83$ GPa and $K_{solid} = 52.6$ GPa.

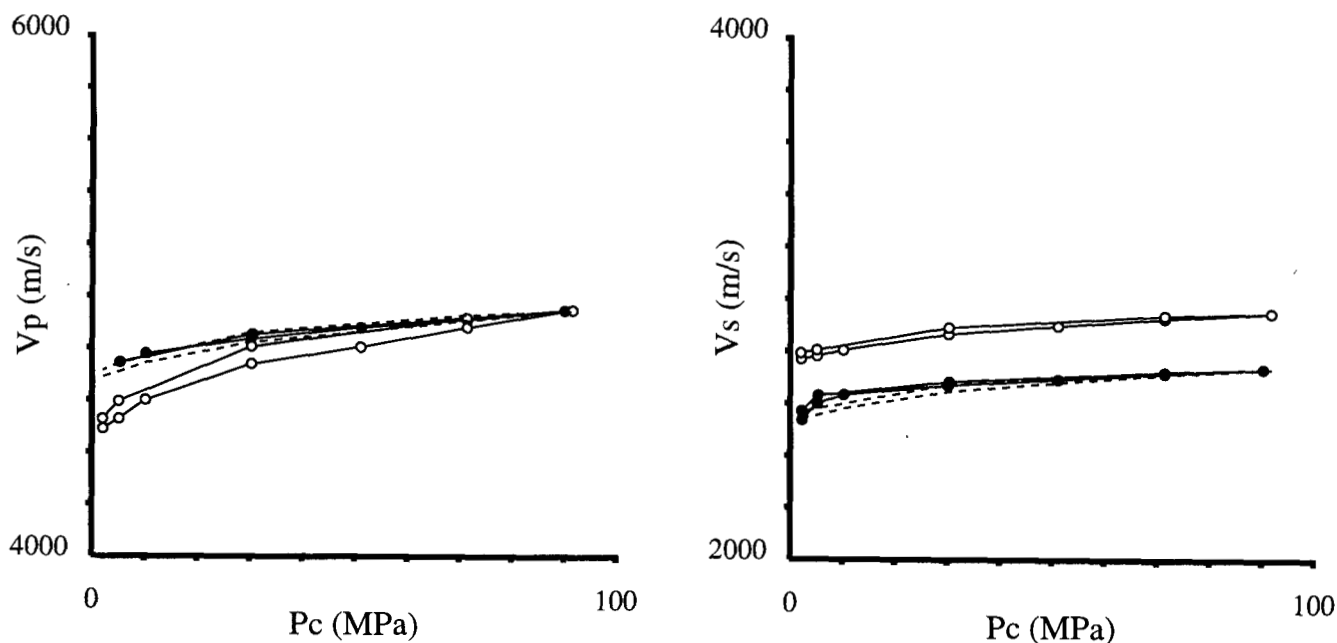


Figure 1b: Compressional and shear velocities as a function of effective confining pressure for argillite plug 1553_s2. Open circles indicate dry and solid circles indicate saturated. The dashed lines are the best fitting model predictions of saturated velocities (based on dry velocities, equations 1a-c, and the bulk properties in Table I), with $\Delta G = 3.06$ GPa and $K_{solid} = 49.0$ GPa.

ever that the velocity/porosity relationship is not strong among any subset of the data other than within metagraywackes from SB-15-D. The relatively high porosity of the SB-15-D argillites may reflect the presence of parting within the foliation, and thus may not be persistent at elevated confining pressures. The degree to which porosity is a controlling factor for velocities remains uncertain.

IV. ELECTRICAL IMPEDANCE

Complex electrical impedance was measured on all samples over a frequency range from 5 Hz to 8 MHz. All samples were saturated with distilled water. Distilled water was chosen to maximize surface conductivity (water/rock interaction) effects as well as to facilitate comparison with electrical impedance measurements during evaporative drying. Most measurements were made at a confining pressure of 10 MPa and a pore pressure of 1 MPa. In general, pressure effects are small compared to intrinsic variation between samples.

The SB-15-D cores have lower resistivities (low frequency) and higher dielectric permittivities (high frequency) than their NEGU-17 counterparts. A summary plot of electrical properties is presented in Figure 3. The strong negative correlation between the real part of the relative dielectric permittivity (κ') and low frequency resistivity (R) appears to be independent of rock type and well. This relationship is not thought to be an intrinsic relationship observed among other rocks, and thus appears to be indicative of composition and/or pore structure of the matrix material from The Geysers.

Electrical impedance versus saturation has been measured on 2 samples of metagraywacke from NEGU-17 (see Figure 4). In these tests, saturated samples with gold electrodes deposited on each end were placed in a dessicator and allowed to dry through evaporation. Complex electrical impedance was measured at various times during the drying process and saturation level was determined by monitoring sample weight before each measurement. An identical test was performed on a sample of Westerly granite for comparison.

For all three samples, the real part of the relative dielectric permittivity (κ') can be fit with a simple linear function of saturation for all saturation levels, with the slope of this linear relationship being a strong function of frequency. This behavior is in contrast to results on sandstones, where saturation effects on (κ') are different at low and high saturations.

In porous sandstones [Knight and Endres, 1990], κ' is very sensitive to water content at low saturations. This sensitivity is thought to reflect the fact that at low saturations, the water is confined to surface films, tight pore spaces, and/or in hydrophilic minerals. This "bound water" appears to result in

significantly higher κ' (per unit volume of water present) than would be expected due to similar amounts of free water. κ' is found to be approximately linear with water content and strongly dependent on frequency in this low saturation ("bound water") regime. In contrast, for porous sandstones at higher saturations, κ' increases more gradually with saturation and is quantitatively consistent with simple mixing laws using the electrical properties of "free" water. This is thought to reflect the fact that at the higher saturations, water is being preferentially added (during saturation) or removed (during drying) from the centers of large pores, where water/rock interactions are not as important.

As seen in Figure 4, the relationship between κ' and saturation is quite different in the metagraywackes. The results on the NEGU-17 metagraywackes are similar to those for Westerly granite and thus may reflect a behavior characteristic of low porosity rocks which is different from that observed in porous sandstones. In these tight rocks, κ' versus saturation is linear over all saturation levels, yet the effect of saturation on κ' is far greater than can be explained using a simple mixing law (assuming the introduction of free water). This may result from the fact that there are no large pores to hold free water. The linear dependence of κ' on saturation indicates a mixing law may be appropriate where the electrical properties of all (or most) of the water is dominated by water/rock interactions (i.e. "bound"). This would indicate that the saturated dielectric permittivities are dominated by water/rock interactions and surface conductivity effects.

V. PERMEABILITY

Permeability as a function of effective confining pressure was measured on four metagraywacke samples from NEGU-17 (see Figure 5). Distilled water was used as the pore fluid. Permeabilities are very low, not exceeding 25 nD even at low effective confining pressures. The pressure effect on permeability is moderate, typically exhibiting an order of magnitude reduction in permeability over the first 30 to 50 MPa in effective confining pressure. Variations between samples is significant and appears correlated (at least qualitatively) with other properties. Although the data-set is limited, low permeability appears correlated with low resistivity, high dielectric permittivity, and high degree of shear modulus reduction with saturation. While it is emphasized that the electrical properties have been measured using distilled water and are thus likely to be dominated by surface conduction and water/rock interactions, the correlations between permeability and electrical properties appear unusual in comparison with data on other rocks.

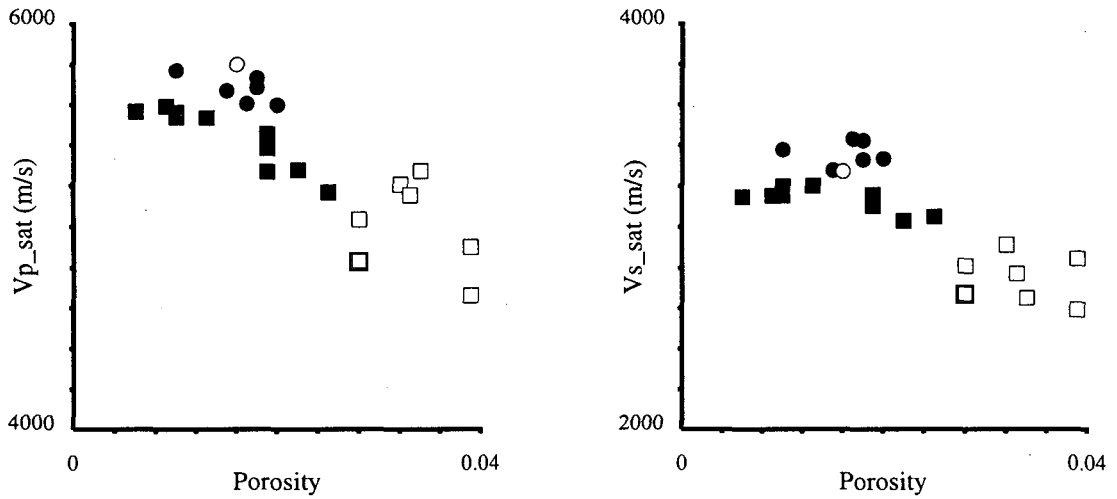


Figure 2: Saturated compressional (V_{p_sat}) and shear (V_{s_sat}) velocities versus porosity for core samples from SB-15-D (squares) and NEGU-17 (circles). Dark symbols indicate metagraywacke and open symbols indicate argillite.

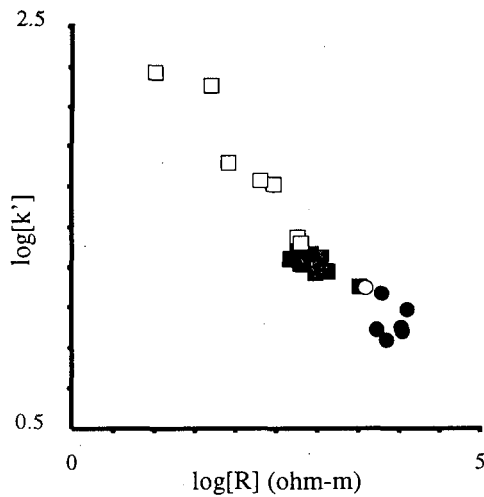


Figure 3: Logarithm of the low frequency resistivity versus logarithm of the real part of the relative dielectric permittivity (at 4MHz) for core samples from SB-15-D (squares) and NEGU-17 (circles). Distilled water was used as the pore fluid. Dark symbols indicate metagraywacke and open symbols indicate argillite.

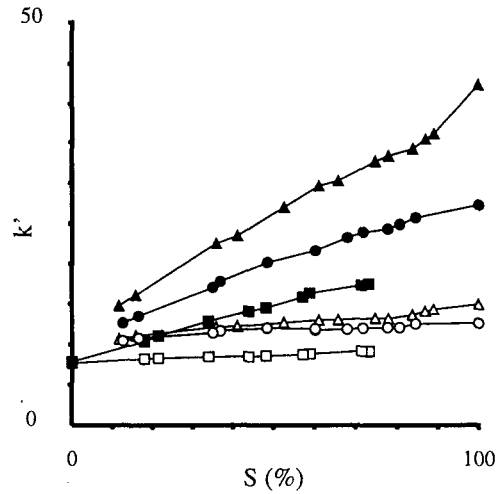
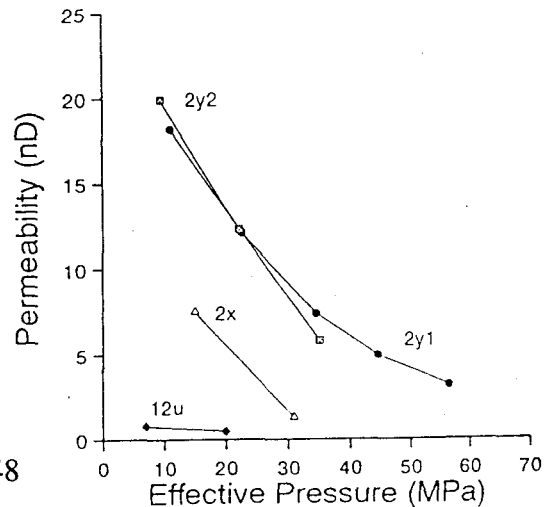


Figure 4: The real of the relative dielectric permittivity (κ') versus saturation (S) for two samples of NEGU-17 metagraywacke (triangles = plug 12u; circles = plug 2x) and one sample of Westerly granite (squares). Open symbols are measurements at 6 MHz and filled symbols are measurements at 60 kHz.

Figure 5: Permeability versus effective confining pressure for 4 samples of metagraywacke from NEGU-17. See Boitnott [1995] for plug descriptions.



VI. DEPTH DEPENDENCE IN SB-15-D

The SB-15-D samples were selected in part to assess whether there are any changes in matrix properties with depth which might be associated with the cap-rock/reservoir boundary. Recently, *Hulen and Nielson* [1995] have suggested that the presence of illite/smectite and chlorite/smectite phases in the veins of the cap-rock are responsible for plugging the flow conduits and thus creating the cap-rock. Smectite content in the vein mineral assemblages is found to decrease significantly in the depth range 375 to 425 m, and thought to reflect the transition from cap-rock to reservoir.

While the samples from SB-15-D tested here span this transition zone, no clear change in velocities or electrical properties is noticeable, suggesting that the matrix in the cap-rock is not appreciably different from the reservoir material. Among metagraywackes, there is some suggestion of higher resistivity, lower dielectric permittivities, and higher acoustic velocities with depth. While these trends are consistent with the loss of smectite with depth (i.e. reflecting a subtle transition from cap-rock to reservoir), they are more likely a result (at least in part) of an apparent negative correlation between porosity and depth which may not play a role in distinguishing cap-rock from reservoir. (see Figure 6).

VII. DISCUSSION

The tests on the SB-15-D matrix material, when compared with identical tests on NEGU-17 matrix, have illustrated that the matrix material is characterized by a number of interesting features. The notably weak pressure effect on acoustic velocities indicates that the porosity is confined to relatively stiff pores and/or mineralized grain contacts and micro-fractures. The effect of saturation on acoustic velocities indicates that saturation produces two dominant effects, a stiffening of the dynamic bulk modulus and a reduction in the dynamic shear modulus. The extent of reduction in shear modulus with saturation is a rather unique characteristic, not being commonly noted among other rock-types.

We have seen in Figure 2 the strong negative correlation between (κ') and (R), which seems to hold for both SB-15-D and NEGU-17 matrix. In addition, from tests on NEGU-17 metagraywacke, we have noted some limited evidence of correlations between electrical properties and permeability. Among metagraywacke samples from NEGU-17, frame weakening appears to correlate with elevated high-frequency dielectric permittivity, and low permeability to liquid water. These correlations may suggest that the pore space may be clogged (to varying degrees) with a hydrophilic clay phase which acts to reduce the permeability while also reducing the electrical resistivity and increasing the dielectric permittivity.

The presence of a hydrophilic clay phase would also be consistent with the observed weakening of the shear modulus with saturation. Importantly, κ' and R show significant correlations with shear velocity reduction upon saturation (see Figure 7). We postulate that the shear weakening with saturation is controlled by composition of the argillaceous material (possibly smectite content). High dielectric permittivity, low resistivity, and large shear weakening would all be consistent with the presence of a hydrophilic clay phase. Following this hypothesis, we postulate that among argillites, composition is the dominant factor controlling both electrical properties and the effects of saturation on velocities. This would suggest that the NEGU-17 argillite, which in comparison to SB-15-D argillites has low resistivity, low dielectric permittivity, and relatively little shear weakening, is compositionally different from the SB-15-D argillites. Along this same line of argument, compositional variations among SB-15-D argillites are apparent from the spread in values among these samples. For metagraywackes, both argillite content (amount) and argillite composition may control the shear weakening and electrical properties. The differences between metagraywackes, both between borehole and within a single borehole, may reflect different argillite composition and/or argillite content. Quantitative petrographic analysis are required in order to test this hypothesis. We suspect that among metagraywackes, dependencies of mechanical, electrical, and transport properties on porosity may also be important, making it difficult to separate variables in many cases.

These observations provide a link between the fundamental physical and transport properties which may be exploited for purposes of reservoir assessment. The observations suggest that a subtle petrographic feature, possibly smectite content, may be a controlling factor for seismic, electrical, and transport properties of the matrix. Attempts to find a signature among the measured properties which reflects the transition from cap-rock to reservoir in SB-15-D have not indicated any dramatic changes in properties associated with the proposed transition zone. However, the matrix properties have been shown to be potentially significant in controlling field scale seismic properties. In addition, matrix porosities are high enough to store significant amounts of water, and thus details of the matrix properties should not be neglected in assessment of reservoir performance.

VIII. ACKNOWLEDGMENTS

This work has been funded by the Geothermal Division of the Dept. of Energy.

IX. REFERENCES

Biot, M. A., Theory of propagation of elastic waves in a fluid-saturated porous solid: I. Low-frequency range, *J. Acous. Soc. Amer.*, 28, 168-178, 1956.

Boitnott, G. N., Laboratory measurements on reservoir rocks from The Geysers geothermal field, in *Proceedings 20th Workshop on Geothermal Reservoir Engineering*, SGP-TR-150, Stanford University, Stanford CA, 107-114, January, 1995.

Hulen, J. B., and D. L. Nielson, Hydrothermal factors in porosity evolution and caprock formation at The Geysers steam field, California

- Insight from The Geysers Coring Project, in *Proceedings 20th Workshop on Geothermal Reservoir Engineering*, SGP-TR-150, Stanford University, Stanford CA, 91-98, January, 1995.

Knight, R., and A. Endres, A new concept in modeling the dielectric response of sandstones - Defining a wetted rock and bulk water system, *Geophysics*, 55, 586-594, 1990.

O'Connell, D. R. H., and L. R. Johnson, Progressive inversion for hypocenters and P wave and S wave velocity structure: Application to The Geysers, California, geothermal field, *J. Geophys. Res.*, 96, 6223-6236, 1991.

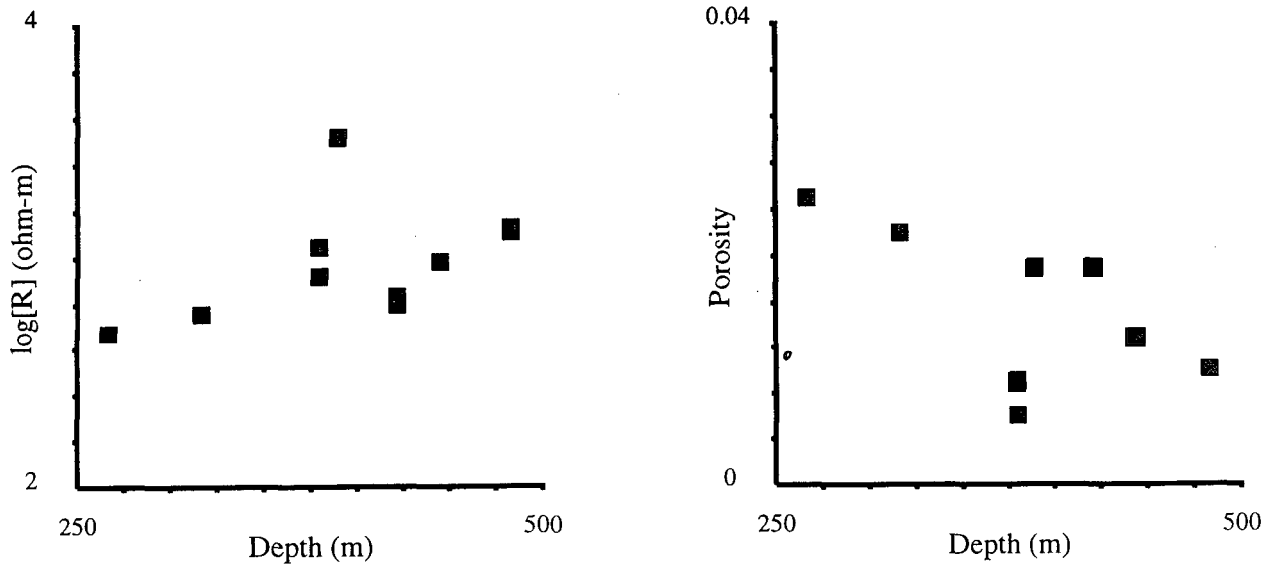


Figure 6: Logarithm of the low frequency resistivity, and porosity, versus depth for metagraywackes in SB-15-D.

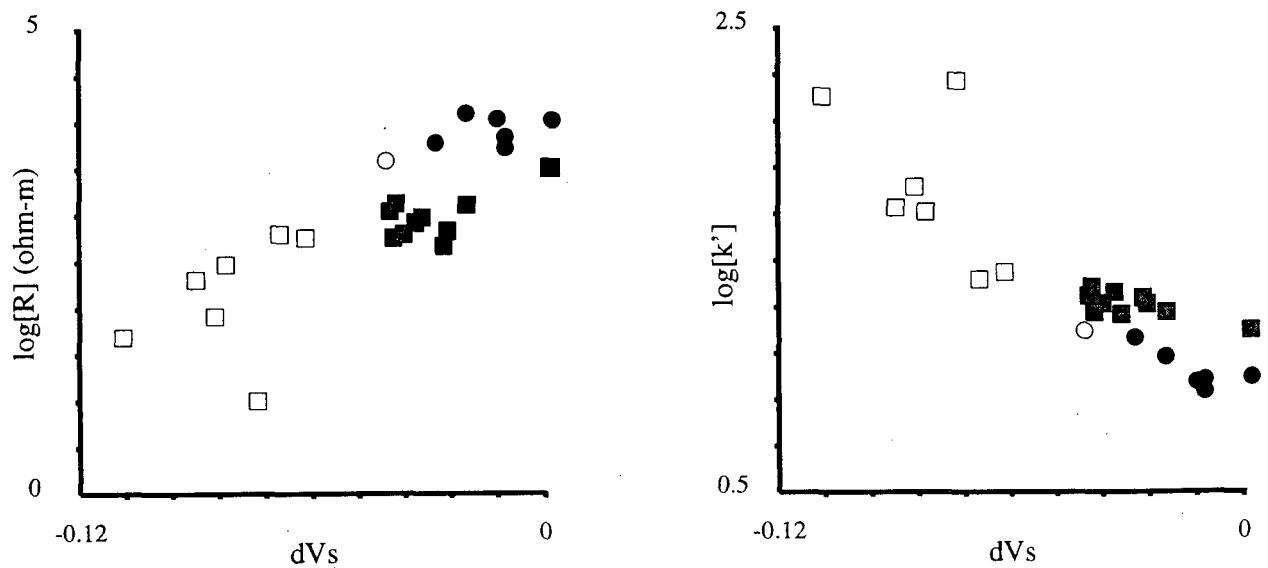


Figure 7: Relative change in shear velocity [$dVs = \Delta V_s / V_{s, dry} = (V_{s, sat} - V_{s, dry}) / V_{s, dry}$] versus the $\log(R)$ and $\log(\kappa')$ for core samples from SB-15-D (squares) and NEGU-17 (circles). Dark symbols indicate metagraywacke and open symbols indicate argillite. Large reduction in shear velocity with saturation correlates with low resistivity and high dielectric permittivity.